LA-UR- 02-0526 c.1

Multi-Sensor Observations of Lightning from Space Using the TRMM and FORTE Satellites

W. L. Boeck

Niagara University, Niagara University, NY, 14109

D. M. Suszcynsky, T. E. Light, A. R. Jacobson

Los Alamos National Laboratory, Space & Atmospheric Sciences Group, MS D466,

Los Alamos, NM 87545

H. J. Christian, S. J. Goodman

Global Hydrology and Climate Center, NASA Marshall Space Flight Center, Huntsville, AL, 35816

D. E. Buechler,

University of Alabama in Huntsville, Huntsville, AL, 35816

J. L. L. Guillen,

Sandia National Laboratories, Sensors and Electronics Dept., MS 0972,

Albuquerque, NM 87185

LOS ALAMOS NATIONAL LABORATORY
3 9338 00864 7488

ABSTRACT

This paper presents coordinated optical and radio frequency observations of an intracloud (IC) lightning flash using instrumentation aboard the Fast On-Orbit Recording of Transient Events (FORTE) and Tropical Rainfall Measuring Mission (TRMM) satellites. The lightning observations, in concert with supplementary radar and imaging data of the associated cloud and precipitation environment, provide a comprehensive high-sensitivity, high time resolution, high-spatial resolution analysis of the flash on both pulse and flash timescales. The collective strengths of the seven-instrument/two-satellite observations are used to remove observational ambiguities that the single instruments can not resolve.

I. INTRODUCTION

Over the last decade, the maturation of satellite-based observations of lightning has been marked by the successful operation of three major sensor packages: the Optical Transient Detector (OTD) sensor operated by the National Aeronautics and Space Administration (NASA) in the mid-1990's, the Lightning Imaging Sensor (LIS) and associated meteorological instrumentation currently operated by NASA aboard the Tropical Rainfall Measuring Mission (TRMM) spacecraft, and a suite of radio frequency (VHF) and optical instrumentation aboard the Fast On-Orbit Recording of Transient Events (FORTE) satellite currently operated by the United States Department of Energy/Los Alamos National Laboratory/Sandia National Laboratories (USDOE/LANL/SNL). Each of these programs has made fundamental advances in the science and engineering of space-based lightning detection [*Boccippio et al.*, 2000, *Buechler et al.*, 2000, *Jacobson et al.*, 2000; *Suszcynsky et al.*, 2001] and each has uniquely excelled in particular aspects of satellite-based lightning detection.

The purpose of the current paper and study is to analyze selected lightning events that were co-observed by both the TRMM and FORTE instrumentation in order to (a) demonstrate the technique of multi-sensor/multi-platform observations of lightning and (b) combine the unique capabilities of each of the TRMM and FORTE instruments to arrive at a more comprehensive event analysis. Comparison of TRMM/FORTE data offers a unique opportunity to demonstrate and exploit the collective strengths of seven state-of-the-art instruments. The unique aspects of each instrument are described in the following paragraphs. More complete instrument descriptions can be found in section II.

The LIS sensor (and its predecessor OTD) is a charged coupled device (CCD) imager in low earth orbit that was launched on November, 28 1997 to advance the state-of-the-art in space-based lightning detection and severe storm monitoring [*Christian et al.,* 1999, *Boccippio et al.,* 2000]. Both the OTD and LIS programs have pioneered the logistics of fielding an operational space-based lightning detection system and have implemented a production data processing and dissemination capability for the user community [*Christian et al.,* 2000]. The particularly low orbit of LIS (350 km) has resulted in the highest spatial resolution (4 km), geolocation accuracy (4 km), and detection efficiency of any space-based optical imager. In addition, LIS is accompanied by an on-board precipitation radar (PR), a visible IR imager (VIRS), and the TRMM microwave imager (TMI), each of which provides additional meteorological information about the cloud environment and precipitation.

The FORTE satellite is a joint LANL/SNL experiment that was launched into a nearly circular 825 km orbit on Aug. 29, 1997. Unlike LIS, the payload is operated in an experimental fashion, routinely re-configured for various data collection campaigns. The instrumentation consists of a two-sensor Optical Lightning System (OLS) and broadband VHF receivers.

The FORTE OLS is comprised of a broadband silicon photodiode detector (PDD) that collects high time resolution (15 μs) waveforms of lightning activity [*Kirkland et al.,* 2001], and an imaging CCD array called the Lightning Location System (LLS), that provides high-spatial resolution imaging and geolocation of events to within a pixel size of 10 km x 10 km [*Suszcynsky et al.*, 2001]. The PDD provides time-resolved optical waveforms that can be correlated with both the LLS and VHF records [*Suszcynsky et al.*, 2000, *Light et al.*, 2001b] and has been used to provide qualitative information about the degree of optical scattering within the cloud [e.g. *Light et al.*, 2001a].

The FORTE VHF receivers can be configured to collect broadband VHF waveforms over various frequency bands within the 20 to 300 MHz frequency range. The VHF power data have proven to be effective for identifying lightning types (e.g. return strokes, leader activity, in-cloud activity) based solely on the frequency-time spectrograms (or power versus time profiles) [*Suszcynsky et al.*, 2000; *Jacobson et al.*, 2000].

Collectively, the FORTE VHF and optical sensors provide a comprehensive dual phenomenology, high-spatial/high-temporal resolution lightning detection capability that can be used to study events on both stroke and flash timescales.

Over the last several years, both the LIS and FORTE programs have each recorded over 10 million lightning events and continue to operate as of the writing of this paper. Although the altitudes (350 km for TRMM and 825 km for FORTE) and orbital inclinations (35° for TRMM and 70° for FORTE) for each satellite differ enough to substantially reduce the number of opportunities to make joint LIS/FORTE observations of lightning events, the orbit crossings are frequent enough to produce one to three lightning storms with overlapping fields-of-view (fov) per month. In general, the TRMM instruments are designed for continuous coverage, high spatial resolution on millisecond time scales. The FORTE instruments are used in campaign mode with individual instrument independently triggering on microsecond time scales. Collectively, the FORTE VHF and optical sensors provide a comprehensive dual phenomenology, high-spatial/high-temporal resolution lightning detection capability that can be used to study events on both stroke and flash timescales. This paper presents a case study of an intracloud (IC) lightning flash and the cloud and precipitation environment of its parent storm as recorded by instruments on both satellites.

II. INSTRUMENTATION AND DATA COLLECTION TECHNIQUES

II.1 TRMM/LIS

The TRMM is a NASA mission designed to monitor and study tropical rainfall and the associated release of latent energy [*Simpson et al.*, 1988]. Three-fourths of the global atmospheric heat energy comes from the release of latent heat by precipitation, of which approximately two-thirds of this precipitation falls in the Tropics. The TRMM orbit ranges from +/- 35° latitude, allowing the spacecraft to fly over a given location at a different time every day over an approximately 42 day cycle [*Kummerow et al.*, 2000]. The TRMM instrument complement includes the TRMM Microwave Imager (TMI), the Visible and Infra-Red Scanner (VIRS), and the first spaceborne Precipitation Radar (PR) as well as the LIS. The instruments are described briefly below; further information on the TRMM instruments onboard can be found *in*[*Kummerow et al.*, 1998].

The separation of electric charge within a thunderstorm is believed to be caused by rebounding collisions between (heavier) graupel pellets and (lighter) smaller ice crystals in the presence of supercooled water droplets [*Latham*, 1981]. This mixed phase region of the thunderstorm where all three of these hydrometeor types coexist is called the charging zone (between the –10° to –20° C levels). The smaller ice particles obtain positive charge and are carried to upper levels, while the larger particles acquire negative charge and stay in the lower portion of the cloud. This mechanism requires a strong updraft, which results in strong vertical development. The various TRMM instruments measure (either directly or indirectly) the vertical distribution of precipitation within storms and their ice content.

1. Lightning Imaging Sensor

The Lightning Imaging Sensor (LIS) is an optical telescope and filter imaging system that investigates the distribution and variability of both atmospheric and cloud-to-ground lightning over the Earth. This lightning sensor consists of a staring imager which is optimized to locate and detect lightning with storm-scale resolution (4 to 7 km) over a large region (600 x 600 km) of the Earth's surface [*Christian et al.*, 1999]. The LIS instrument consists of a front-end optical assembly, a fixed-position CCD focal plane assembly with drive electronics and a real time event processor (RTEP) module. The optics are filtered at 777.4 nm and provide an 80 x 80 degree square fov. The LIS design uses four filtering techniques to allow lightning detection in the presence of sunlight that is reflected and scattered from cloud tops. Spatial filtering is accomplished by the design choice matching the 80 degree optical FOV with the 128 by 128 pixel array. This design allows optical energy from a typical cloud-top area to be focussed onto a single pixel. A narrow-band interference filter centered on a strong oxygen triplet in the lightning spectrum provides spectral filtering. The time domain filtering uses a short integration time of 2 ms to capture an entire optical pulse while minimizing the background integration of reflected sunlight. Event filtering uses a pixel by pixel background memory to remove the content of the slowly varying background scene while retaining optical pulses. The background scene is read out every 60 to 90 seconds. In the daytime background images, clouds, land and water features can be identified. The pixel integration time is too short to capture useful images at night.

LIS pixel data is organized into a hierarchy of storm areas, flashes, optical frame groups and individual pixels by a spatial-temporal grouping algorithm [*Christian et al.* 2000] that finds the individual pixel events that are clustered in location and time. NASA chose the Hierarchical Data Format (HDF) for all

data products from the Earth Observing System. There is one HDF file for each TRMM orbit, which starts at the southernmost point of the satellite orbit. The LIS file contains a hierarchy of data products, summary data and images and the details of the ancillary data. The HDF file structure contains forward and reverse links connecting each storm area to the individual flashes for that storm. Each flash is linked to all of its optical groups and in turn to each item of pixel data including the raw data for each flash. Ancillary data is provided in sufficient detail to recompute the clustering or even use an alternate clustering algorithm.

The TRMM Satellite travels a distance of 7 kilometers every second (nearly 16,000 miles per hour) as it orbits the Earth, thus allowing the LIS and other instruments to observe a point on the Earth or a cloud for almost 90 seconds as it passes overhead. Despite the brief duration of an observation, it is long enough to estimate the flashing rate of most storms. The LIS instrument records the time of occurrence, measures the radiant energy, and determines the location of lightning events within its field-of-view.

2. Precipitation Radar

The PR is an active system operating at 13.8 GHz, recording energy reflected from atmospheric and surface targets. The PR has a swath width of 215 km and a footprint of 4.3 km at nadir. The PR provides measurements of the three-dimensional structure of rainfall, allowing classification of rainfall into stratiform or convective based on the absence/presence of a bright band signature in the vertical. The PR can observe precipitation over land regions, where passive microwave precipitation estimation is less accurate. Radar reflectivity (~40 dBZ) values at altitudes above the -10° C level would indicate a likely lightning producing storm [*Dye et al.,* 1989].

3. TRMM Microwave Imager

The TMI is a 9 channel passive microwave radiometer which measures the amount of radiation emitted from the Earth's surface and atmosphere. The radiometer measures the upwelling radiation at 10.7, 19.4, 21.3, 37.0, and 85.5 GHz, which are then converted to brightness temperatures via Planck's radiation law. Each channel has one vertically and one horizontally polarized channel, except for the 21.3 GHZ channel which only has a vertical polarization. The swath width of the TMI is 785 km with footprints ranging from ~35 km^2 at 85.5 GHZ to ~2330 km^2 at 10.7 GHz [*Kummerow et al.*, 1998]. The upwelling radiation responds to the phase, vertical distribution, density, concentration, and size of hydrometeors within the TMI footprint. The response is different for each wavelength. For example, the observed brightness temperature is reduced by scattering of upwelling radiation by precipitation size ice at both 37 GHz and 85.5 GHz [*Wu and Wienman*, 1984]. Therefore, low brightness temperatures at 35 and 85.5 GHz are indicative of precipitation sized ice such as found in deep convection. A relationship between cold 85.5 and 37 GHz brightness temperatures and LIS lightning observations has been reported *[Blyth et al.*, 2001].

4. Visible/Infrared Scanner

The VIRS measures radiance from the visible through the infra-red (.63, 1.6, 3.75, 10.8, 12.2 μm) portion of the spectrum. The VIRS swath width is 720 km with a nadir resolution of 2.2 km. The VIRS data is used to study precipitation using visible and IR techniques first derived from geostationary measurements. Various techniques have been used with observations from geostationary satellites to estimate precipitation [*Barrett and Martin*, 1981]. These typically involve examination of the visible

and/or IR imagery to derive spatial and temporal distribution of cloud top temperature and cloud brightness to deduce the distribution and intensity of surface precipitation beneath these clouds. In general, the colder cloud top temperatures indicate more vigorous clouds that result in more precipitation and more lightning activity.

B. Fast On-Orbit Recording of Transient Events

FORTE flies in a nearly circular, 70° inclination orbit of approximately 825 km altitude with an orbital period of about 100 minutes. The spacecraft system and the sensors has been described [*Roussel-Dupre et al.*, 2001].

1. VHF Receiver

The two FORTE VHF receivers used in this study can each be independently configured to cover a 22-MHz sub-band in the 26 - 300 MHz frequency ranges. For this study, one receiver was chosen to span the 26 - 48 MHz range and the other spanned the 118 - 140 MHz range. The instruments were typically configured to collect 20480 samples in a 400 μs record length resulting in a time resolution of 20 ns. Data collection is triggered off the lower (26 - 48 MHz) band receiver when the amplitude of its detected signal exceeds a preset noise-riding amplitude threshold in at least five of eight 1 MHz wide sub-bands distributed throughout the 22-MHz bandwidth [*Jacobson et al.,* 1999,2000]. This triggering technique allows the instrument to trigger on and detect weak lightning signatures in the presence of some interfering man-made carriers. Retriggering can occur after only a few microsecond delay allowing the instrument to record extended multi-record signals with essentially zero dead-time. The "field-of-view" of the VHF receivers is centered on the sub-satellite point and is determined by the antenna pattern; the

3-dB attenuation contour of the antenna response approximates a circle of about 1200 km diameter on the earth and was chosen to roughly correspond to the 80° field-of-view of the PDD.

2. FORTE Photodiode Detector

The PDD is a broadband (0.4 - 1.1 μm) silicon photodiode detector that collects amplitude versus time waveforms of optical transients [*Kirkland et al.* 2001], particularly those associated with individual strokes/pulses of a lightning flash. The instrument has an 80° fov, which translates into a footprint of about 1200-km diameter for an 825 km altitude orbit. In the "autonomous" mode used for this study, the instrument collects 1.92 ms long waveforms with 15 μs time resolution. Data collection is amplitude-threshold triggered, with a background-riding threshold, and with a requirement that the signal amplitude exceed the amplitude threshold for five consecutive samples (75 μs) before a trigger occurs. This protocol minimizes false triggers due to energetic particles. The PDD provides 12-bit sampling with a piece-wise linear dynamic range covering four orders of magnitude and a sensitivity of better than 10^{-5} W/m^2. The dead time between successive PDD records is approximately one record length (1.92 ms). The trigger times of both the PDD and LLS records are GPS time-stamped to a precision of 1 μs.

3. FORTE Lightning Location Sensor

The LLS is a 128 x 128 pixel CCD array designed to identify and locate lightning flashes to a 10 x 10 km resolution. The LLS instrument consists of an optical assembly, a fixed-position CCD focal plane assembly with drive electronics and a SNL-developed operations and signal processing module for lightning data discrimination [*Suszcynsky et al.* 2001]. The optical and CCD assemblies are identical to those used on the LIS developed by NASA. The LLS typically operates in the normal pixel event mode

where a pixel event is recorded whenever any given pixel exceeds an amplitude threshold level for less than 3 consecutive frames (1 frame equals 2.5 ms of integration). Adding a background trigger offset to the average background amplitude sets the threshold level. When an LLS pixel event is detected, the LLS processing algorithm records the frame time of the event, and the address and amplitude (detected energy density) for each pixel that participates in the event. The LLS has a typical dead time between triggers of 2.5 ms (one frame integration interval).

RESULTS

Shortly after 12:05.11 UTC on July 16, 1998, during local night, both FORTE and TRMM observed the same lightning flash at a location –5.60 latitude and 161.86 longitude, which is east of the Solomon Islands. LLS viewed this location from 12:04:09 until 12:08:16. Because TRMM flies at a lower altitude, LIS observed this storm from 12:04:15 until 12:05:52, a total of 84 seconds. At the time of the flash, the target range for TRMM was 366 km and for FORTE 1016 km. There is no information in the LIS background scene because it was a nighttime scene.

The HDF file [Christian et al., 2000] produced by LIS is the starting point of this analysis. The LIS data is used to identify the location and the optical pulses of individual flashes from a lightning storm. FORTE data collected in the same time interval is compared to LIS flash level data to determine if both platforms have recorded the same flash. In this overpass, LIS detected only one lightning storm, which produced a single flash while in the field of view. LIS recorded data in 272 pixels spread out over 33 distinct optical frames. The LLS was at a range about 3 times larger than LIS and received about an order of magnitude less optical energy from this flash. The LLS triggered once during the flash

registering a 1-pixel event. The LLS geolocated the flash at –5.60 latitude and 161.86 longitude while the LIS geolocated it at a latitude of -5.61 and a longitude of 161.723. The good agreement in location between LLS and LIS, and the characteristic temporal coincidence between LLS, PDD and the VHF waveforms, removes any ambiguity regarding the source of the optical and simultaneous VHF energy recorded by FORTE. The LIS also measured the footprint size, which varied from 17 square kilometers to 384 square kilometers at various times during the flash.

Figure 1 summarizes the detection of the flash by the TRMM and FORTE lightning detectors

The top panel in figure 1 presents the time development of this flash from 12:05.11.8 to 12:05.12.1 UTC. The gray bars plot the radiance observed by LIS in μJ/str/sqm/micron . The flash starts at 12:05:11.873 with a quasi-continuous illumination of 33 ms duration with only a single 2 ms gap. This gap and the larger gaps that follow may be instances when the radiance dropped below the LIS threshold. The eight diamonds plotted on the upper diagram show the times of the FORTE VHF triggers associated with the flash. These VHF records are less than one half of a millisecond in length.

FORTE detected 15 VHF triggers in all during the time interval displayed in figure 1. Of these triggers , the eight shown in figure 1 were conclusively associated with the particular flash under study by using a technique that associates triggers with similar values of slant total electron content (TEC) with the same storm [*Jacobsen et al.,* 1999]. The assumption is that VHF signals originating at the same location will propagate along the same ray through the ionosphere, thereby experiencing the same amount of dispersion due to TEC.

The middle panel in figure 1 shows100 ms at the beginning of the flash on an expanded time scale from 12:05.11.85 to 12:05.11.95 UTC. The data range is delimited by triangles in the top panel. The output

of the PDD is superimposed on the gray LIS data bars and the VHF diamonds. After adjusting the time scale for each data stream, data time is plotted as the UTC time at the source location. The PDD amplitude is multiplied by a factor of 10000 to produce a convenient overlay of the LIS data in the plot

There is good temporal agreement between the integrated optical record produced by LIS and the detailed pulses captured by PDD. The general characteristics of coincident imager/photodiode detection of lightning activity has been presented in detail [*Suszcynsky et al.*, 2001].

The lowest three panels in figure 1 show a detailed timing comparison of three coincident VHF/ PDD pairs of waveforms that are marked A, B, C in the middle panel. The delay of the optical pulse with respect to the VHF pulse, "delta t", is primarily due to multiple scattering of the light by snow and ice crystals in the upper part of the storm. The delays can be calculated by the technique described in [*Light et al.*, 2001b] for distinct in-cloud events (see discussion section) and are indicated on the top of two of the panel. The VHF signal consists of distinct impulsive events that are barely resolved on these millisecond scale plots. The spatial and temporal agreement of the LLS and LIS triggers in concert with the characteristic timing relationships between the LLS, PDD and VHF waveforms verify that all four instruments recorded the same lightning flash.

Examination of impulsive VHF power plots such as those in figure 1 frequently finds pairs of VHF pulses that are similar in shape and detail. The first pulse is interpreted as an in-cloud impulsive VHF emission that transits along a direct path to the satellite; the second pulse is a reflection of the source pulse from the earth's surface to the satellite. The delay between the source pulse and its reflection is given by the difference in propagation time due to the differing propagation path lengths. A knowledge of the source location, the satellite location, and the delay between the source and reflected pulses

completely defines the detection geometry and results in an absolute estimate of the height of the VHF source [*Jacobson et al.*, 1999, *Tierney et al.*, 2001]. The Y coordinate of the VHF diamonds plotted in the upper two panels of figure 1 gives the calculated height of the VHF sources of this flash. Individual heights range from 9.25 km to 13.13 km on the scale at the right side of the figure.

Figure 2 is a plot on a microsecond scale of the VHF energy in the C VHF/PDD pair. Two peaks, that are very similar in detail, dominate the plot. The peak at the 100 microsecond mark is the event that triggered the VHF recorder. The reflected peak shows the same detailed splitting as the first. The measured time delay of 67 microseconds can be used with the range of 1016 km to determine that the altitude of the VHF source was 12.9 km. The LIS measured the footprint of the flash as it expands from 97 sq. km to 240 sq. km. at this time. The source height for the other two examples in figure 1 is 9.5 km.

Figure 3 presents apparent brightness temperature data from the TMI instrument on TRMM. These measurements were taken within 20 seconds of the time of the lightning flash. The outlines show the location of several of the Solomon Islands. The red slash marks the source location for lightning (location Z, uncorrected for parallax). The black line illustrates the width of the PR scan. This line also shows the location of the vertical cross section displayed in the next figure. The warm ocean temperatures are displayed in blue. The green pixels show the location of precipitating clouds The orange pixels imbedded in the green areas mark cold cloud cores where precipitation sized ice causes a large apparent temperature depression. The overall lightning rate for the entire cluster of storms is low. There are over a dozen storms with cold cloud tops, but only one produced a lightning flash while within the LIS fields of view.

The upper panel in figure 4 plots the infrared and apparent microware brightness temperature profiles along the black line in figure 3 The lower panel of figure 4 presents a radar vertical profile along the

same cross section . There is some misalignment between the upper and lower panels because the cross track distance in the upper panel was not corrected for parallax. The VHF source elevations plotted in figure 1 range from 9.3 km to 13.1 km. In the RADAR profile there is significant precipitation producing a 25 dbz return at 9 km and direct evidence of a 15 dbz return from 13 km near the + 100km mark.. Additional evidence of the cloud top height is provided by VIRS, which recorded an IR brightness temperature around 200 K. There large depression of the microwave temperature is diagnostic of ice in a cold storm core.

DISCUSSION

The simultaneous observation of a lightning flash and its storm environment by seven of the satellite instruments aboard TRMM and FORTE can remove ambiguities that the individual instruments can not resolve. For example, the TMI and PR instruments can unambiguously detect and identify each of the many convective cells, with ice signatures, that often occur within each fov, but they cannot determine which storms are producing lightning. Although the VIRS and TMI show that there are several anvil clouds in this field of view, the LIS imager observed lightning from one of the storm locations. Conversely, imagers such as LIS and LLS identify and geolocate lightning producing storms but cannot detect non-electrically active convective regions without the aid of a cloud imager such as VIRS or a LIS daytime background scene. As a second example, stand-alone optical measurements have not reliably resolved the ambiguities in distinguishing between cloud to ground (CG) lightning and intracloud (IC) lightning. Conversely, single-platform satellite VHF measurements can effective discriminate between CG and IC lightning but can not pinpoint the location of the source.

The case study presented demonstrates the collective strength of all six instruments in providing high-sensitivity, high-time resolution, high-spatial resolution detection of lightning activity at both pulse and flash timescales, and in concert with supplementary radar and imaging data of the associated cloud and precipitation environment. For example, using the full instrument suite available in our study, the flash can be reliably identified as an IC flash based on three features:

(1) Each of the eight VHF power profiles in the flash are comprised of impulsive emissions with intra-pulse spacing implying source altitudes in the 9 -13 km range. The RADAR cross-section from PR proves the existence of precipitation at the altitudes derived by the VHF source height analysis.

(2) there are no return stroke signatures in the VHF power profiles, e.g. no VHF signatures of leader activity or return stroke attachment processes [*Suszcynsky et al*, 2000], and

(3) the temporal relationships between the four VHF/PDD waveform pairs shown in Figure 1 are more consistent with an in-cloud source [Light et al, 2001b] rather than a ground (CG) source. The VHF/PDD correlation times, Δt_{corr}, for each of the four VHF/PDD waveform pairs are consistent with intracloud activity (~ tens of μs with the optical signature occurring slightly later due to scattering processes as opposed to the ~ 100 μs correlation times typically found associated with return strokes.). Although Δt_{corr} is primarily a function of the density and distribution of water droplets along the source/satellite line-of-sight, Monte Carlo modeling has shown that the values cannot be used to deduce specific characteristics of the cloud because of the uncertainty of the source function and the complex nature of the scattering environment [*Light et al.*, 2000a]. Nonetheless, the reproducibility of Δt values for physically coincident VHF/PDD waveform pairs is robust enough to reliably distinguish between physically coincident events and those that are incidentally coincident in time but not space.

The LIS and the LLS were designed to integrate for 2 or 2.5 ms to match the width of individual scattered lightning optical pulses. This set of coincident PDD records demonstrates the validity of that design decision. Two out of the five PDD waveform plots show overlapping optical pulses. The continuous light recorded by LIS can be interpreted as the integrated result of overlapping or nearly overlapping optical pulses. The location of three VHF diamonds during a time gap in the LIS record is evidence that the electrical discharge activity of this flash is continuing but with optical output temporarily below the threshold of the LIS and LLS detector. Altogether, the evidence shows that this IC was dominated by a quasi-continuos series of discharges in the upper part of the cloud.

In summary, multi-phenomenology, multi-sensor observations of lightning from space using the FORTE and TRMM spacecraft provide a surprisingly detailed picture of lightning phenomenology on both stroke (pulse) and flash time scales. Collectively, the sensors allow us to detect, locate, measure, analyze and classify lightning on a global basis and provide good argument for outfitting future satellite-based global lightning monitors with optical imaging and VHF sensors.

ACKNOWLEDGMENTS

The authors would like to thank Diane Roussel-Dupre of Los Alamos National Laboratory, Dennis Boccippio of NASA/MSFC, Doug Mach of UAH, Jeff Green and Bill Myre of Sandia National Laboratories and the rest of the FORTE and TRMM Science and Operations Teams for essential

discussions, comments, and technical support during this study. This work was supported by the United States Department of Energy.

REFERENCES

Barnes, W. L., R. A. Barnes, A. W. Holmes, Characterization and Calibration Results from the Visible and Infrared Scanner (VIRS) for the Tropical Rainfall Measurement Mission (TRMM), SPIE 2957, 266-276,1996.

Barrett, E.C., and D.W. Martin, *The use of satellite data in rainfall monitoring*. Academic Press, 340 pp.,1981.

Blyth, A.M., H.J. Christian, K. Driscoll, and J. Latham, Determination of ice precipitation rates and thunderstorm anvil ice contents from satellite observations of lightning, Accepted for publication in *Atmospheric Research*, 2001.

Boccippio, D.J., K.Driscoll, W. Koshak, R. Blakeslee, W. Boeck, D. Buechler, H. Christian, S. Good man, The Optical Transient Detector (OTD): Instrument characteristics and cross-sensor validation, *J. Atmos. Oceanic. Tech.*, **17**, 441-458, 2000

Buechler, D. E., K. Driscoll, S. Goodman, H. J. Christian, Lightning Activity within a Tornadic Thunderstorm observed by the Optical Transient Detector (OTD), *Geophys. Res. Lett.*, **27**, 2253-2256, 2000.

Christian, H. J., R. J. Blakeslee, S. J. Goodman, D. A. Mach, LIS Algorithm Theoretical Basis Document, *http://eospso.gsfc.nasa.gov/atbd/listables.html,* Feb 1, 2000

Christian, H. J., R. J. Blakeslee, S. J. Goodman, D. A. Mach, M. F. Stewart, D. E. Buechler, W. J. Koshak, J. M. Hall, W. L. Boeck, K. T. Driscoll, and D. J. Bocippio, The Lightning Imaging Sensor, Proceedings of the 11th International Conference on Atmospheric Electricity, Guntersville, Alabama, June 7-11, 1999, pp. 746-749.

Christian, H. J., Optical Detection of Lightning from Space, Proceedings of the 11th International Conference on Atmospheric Electricity, Guntersville, Alabama, June 7-11, 1999, pp.715-718.

Dye, J.E., W.P. Winn, J.J. Jones, and D.W. Breed, The electrification of New Mexico thunderstorms. Part 1.: Relationship between precipitation development and the onset of electrification. *J. Geophys. Res.*, **94**, 8643-8656,1989.

Jacobson, A. R., S. O. Knox, R. Franz, D. C. Enemark, FORTE observations of lightning radio-frequency signatures: capabilities and basic results, *Radio Sci.*, ***34***, 337-354, 1999.

Jacobson, A. R., K. L. Cummins, M. Carter, P. Klingner, D. Roussel-Dupre, S. O. Knox, FORTE radio-frequency observations of lightning strokes detected by the National Lightning Detection Network, *J. Geophys. Res. –Atmos.*, **105**, 15653-15658, 2000.

Kirkland, M. W., David M. Suszcynsky, R. Franz, J. L. L. Guillen, and J. L. Green, Optical observations of terrestrial lightning by the FORTE satellite photodiode detector, in press, *J. Geophys. Res. - Atmos.*, 2001.

Kummerow, C., W. Barnes, T. Kozu, J. Shiue, J. Simpson, The Tropical Rainfall Measuring Mission (TRMM) Sensor Package. *J. Atmos. Oceanic Technol.*,**15**, 809-817, 1998.

Kummerow, C., J. Simpson, O. Thiele, W. Barnes, A.T.C. Chang, E. Stocker, R.F. Adler, A. Hou, R. Kakar, F. Wentz, P. Ashcroft, T. Kozu, Y. Hong, K. Okamoto, T. Iguchi, H. Kuroiwa, E. Im, Z. Haddad, G. Huffman, B. Ferrier, W.S. Olson, E. Zipser, E.A. Smith, T.T. Wilheit, G. North, T. Krishnamurti, and K. Nakamura, The status of the Tropical Rainfall Measuring Mission (TRMM) after two years in orbit. *J. Appl. Meteor.*, **39**, 1965-1982, 2000.

Latham, J., 1981: The electrification of thunderstorms. The Symons Memorial Lecture 1979, *Q. J. Roy. Met. Soc.*, **107**, 277-298.,1979.

Light, T. E., D. M. Suszcynsky, M. W. Kirkland, and A. R. Jacobson, Simulations of lightning optical waveforms as seen through clouds by satellites, in press, *J. Geophys. Res. –Atmos.*, 2001a.

Light, T. E., D. M. Suszcynsky, and A. R. Jacobson, Coincident radio frequency and optical emissions from lightning observed with the FORTE satellite, *J. Geophys. Res. – Atmos.*,**106**,28223-28231, 2001b.

Tierney, H. E. ; Jacobson, A. R. ; Beasley, W. H. ; Argo, P. E. , Determination of source thunderstorms for VHF emissions observed by the FORTE satellite *Radio Sci.* , ***36*** , 79-85, 2001

Roussel-Dupre, D., P. Klingner, L. Carlson, R. Dingler, D. Esch-Mosher, Four Years of Operations and Results with FORTE, AIAA, Space 2001 conference.

Simpson, J., R. F. Adler, G. R. North, 1988: A Proposed Tropical Rainfall Measuring Mission (TRMM) Satellite. Bulletin of the American Meteorological Society, **69**, 3, 278-278, 1998.

Suszcynsky, D. M., M. W. Kirkland, A. Jacobson, R. Franz, S. Knox, J. L. Guillen, J. Green, FORTE Observations of Simultaneous RF and Optical Emissions from Lightning: Basic Phenomenology, *J. Geophys. Res. - Atmos.*, **105**, 2191-2201, 2000.

Suszcynsky, D. M., T. E. Light, S. Davis, J. L. Green, J. L. L. Guillen, W. Myre, Coordinated Observations of Optical Lightning from Space using the FORTE Photodiode Detector and CCD Imager, in press, *J. Geophys. Res. –Atmos.*, 2001.

Wu, R., and J.A. Weinman, Microwave radiances from precipitating clouds containing aspherical ice, combined phase, and liquid hydrometeors. *J. Geophys. Res.*, **89**, 7170-7178,1984.

Captions

Figure 1. Plot of lightning data versus source time.
Upper panel shows LIS radiance data. Diamonds mark times of VHF data. Data between triangles is expanded in middle panel
Middle panel compares LIS and PDD data on an UTC time scale. Diamonds mark height of VHF sources. PDD data A, B, and C are expanded in the lowest panel.
Lower panels compare PDD and VHF data for examples A, B and C. PDD data marked with small circles.

Figure 2. Expanded plot of VHF example C showing source and reflected pulse.

Figure 3. TRMM plot displaying TMI data. The red slash marks the source location for lightning (location Z). The black line marks the location of the vertical cross section in the next figure.

Figure 3. TRMM data displaying PR, TMI and VIRS data. Storm location marked by C.

Figure 4. Cross section data from TMI, VIRS and PR as marked in Figure 3. The upper panel plots apparent brightness temperatures at an infrared and microwave frequency. The lower panel is a vertical section of the precipitation. The lightning source is near the Z marker.

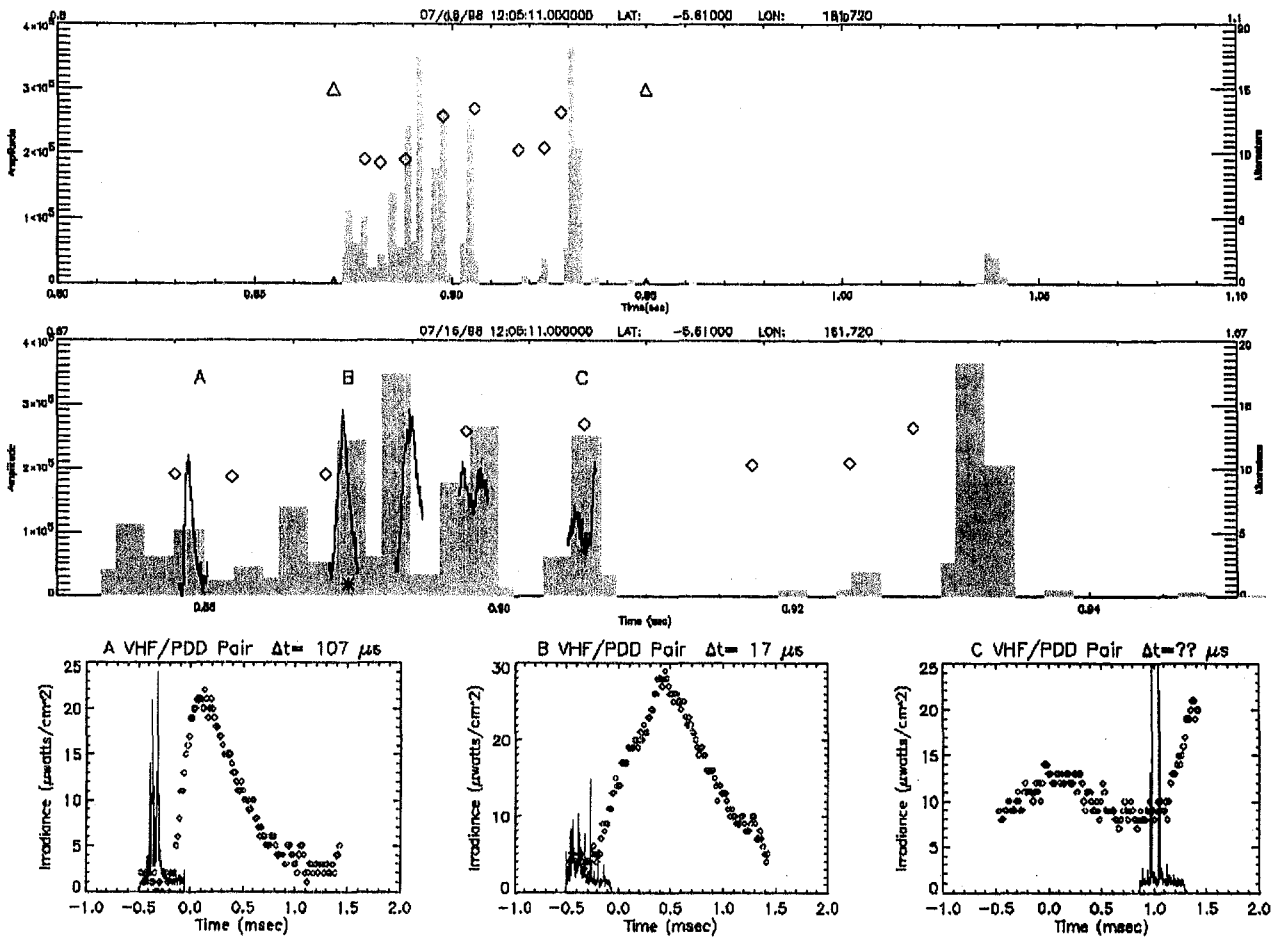

Figure 1. Plot of lightning data versus source time.
Upper panel shows LIS radiance data. Diamonds mark times of VHF data. Data between triangles is expanded in middle panel
Middle panel compares LIS and PDD data on an UTC time scale. Diamonds mark height of VHF sources. PDD data A, B, and C are expanded in the lowest panel.
Lower panels compare PDD and VHF data for examples A, B and C. PDD data marked with small circles.

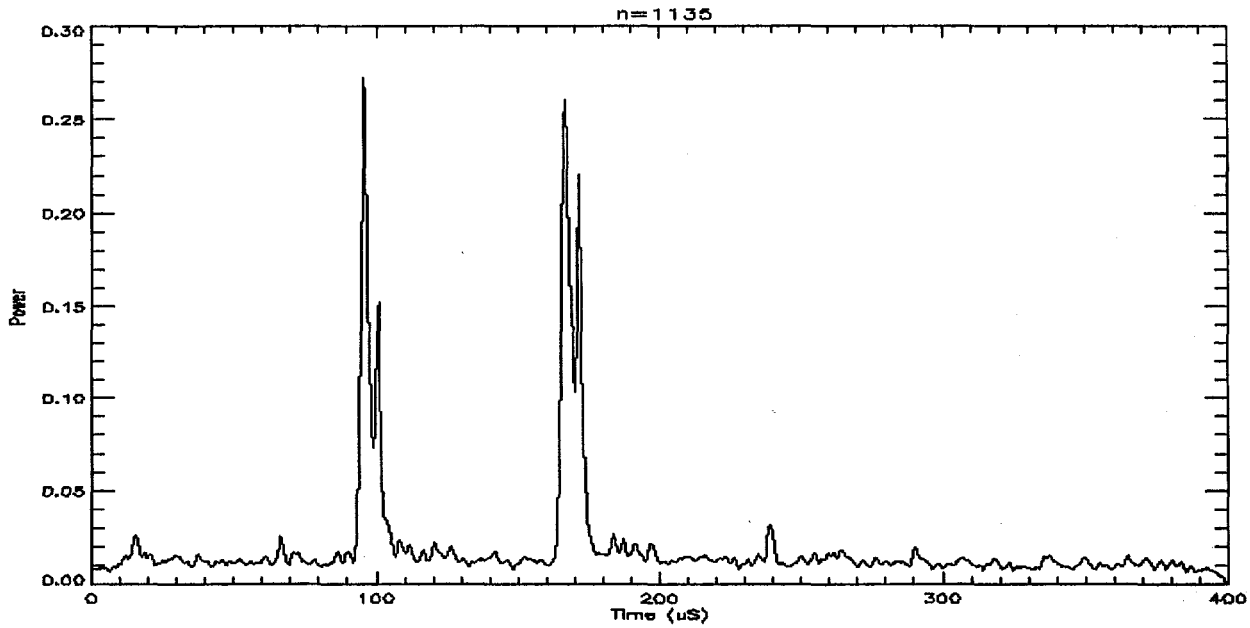

Figure 2. Expanded plot of VHF example C showing source and reflected pulse.

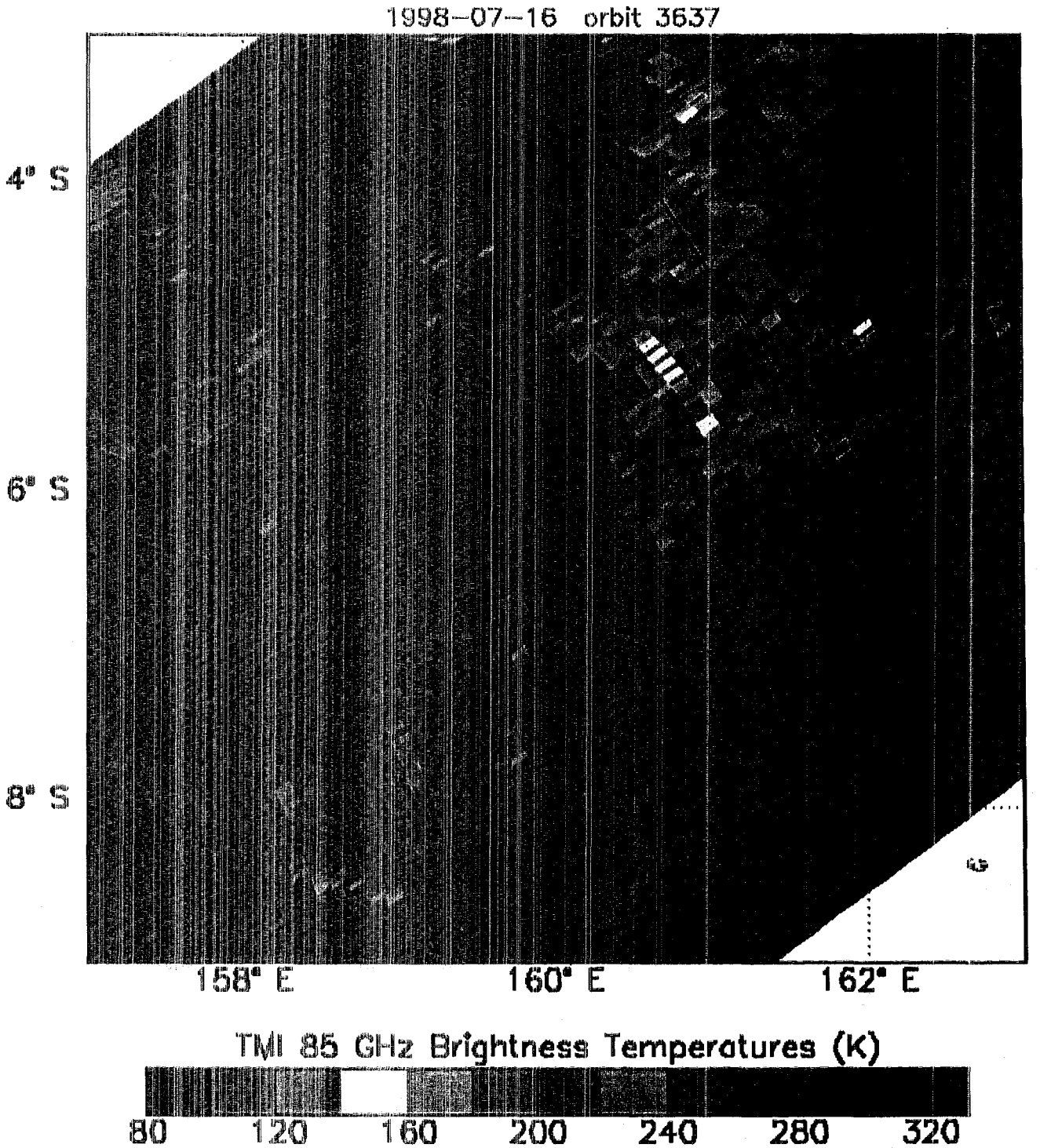

Figure 3. TRMM plot displaying TMI data. The red slash marks the source location for lightning (location Z). The black line marks the location of the vertical cross section in the next figure.

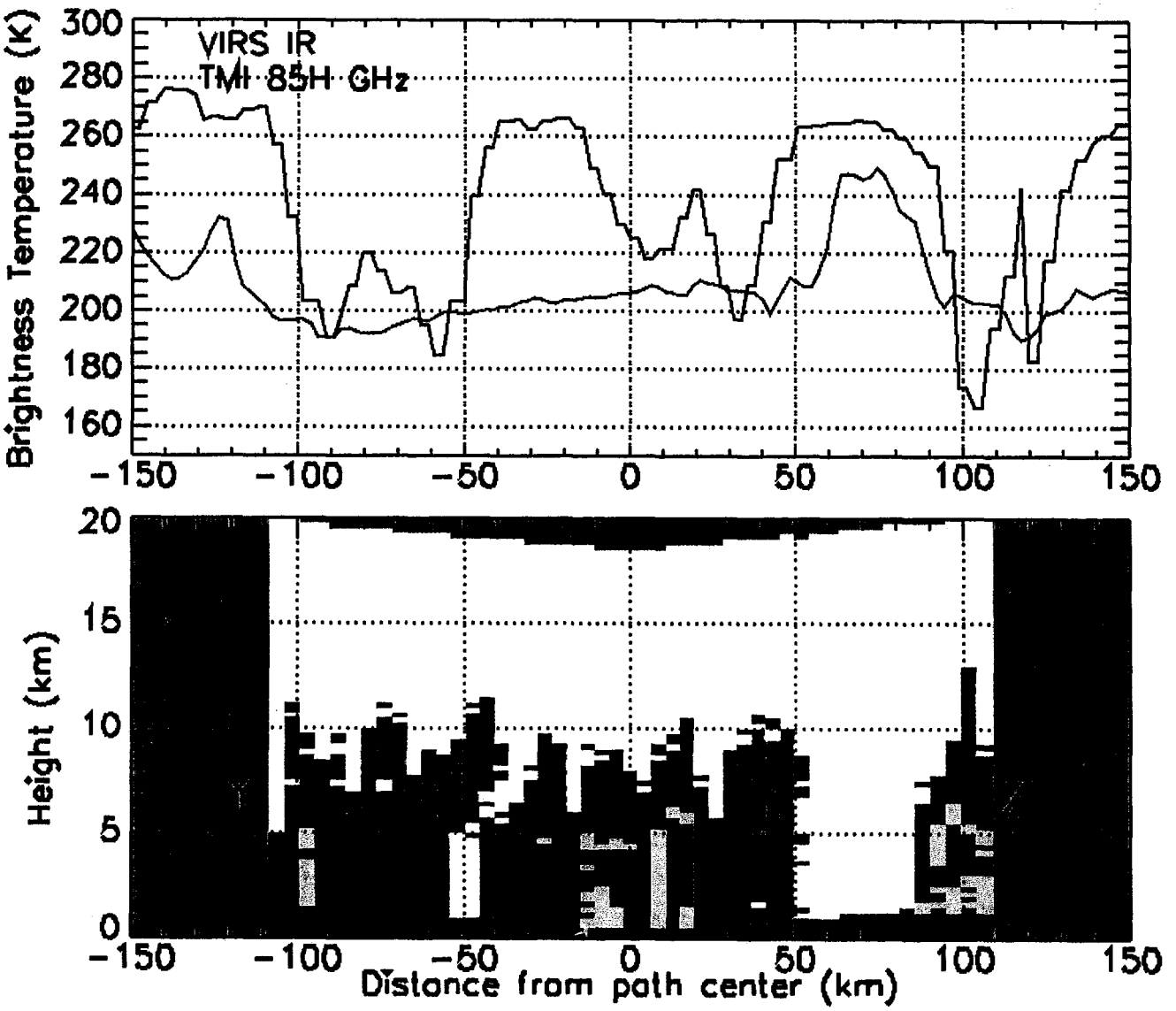

Figure 4 Cross section data from TMI, VIRS and PR as marked in Figure 3. The upper panel plots apparent brightness temperatures at an infrared and microwave frequency. The lower panel is a vertical section of the precipitation. The lightning source is near the Z marker.